ELSEVIER

Lithos 55 (2001) 115–124

LITHOS

www.elsevier.nl/locate/lithos

Radiogenic isotopes in fluid inclusions

Igor M. Villa*

Isotopengeologie, Mineralogisch-Petrographisches Institut, Universität Bern, Erlachstrasse 9a, 3012 Bern, Switzerland

Received 20 August 1999; accepted 28 April 2000

Abstract

Radiogenic isotopes studied in fluid inclusions are still a limited field, with great potential for expansion as analytical techniques improve. The main limitation for Sr, Ar and He isotope work is the very small number of radiogenic atoms produced in a typical fluid inclusion. The requirements to analysts are correspondingly high. Examples show that isotopic tracing on fluid inclusion fluids can be a decisive tool in solving geological problems.

Keywords: Fluid inclusions; Ar isotopes; He isotopes; Sr isotopes

1. Introduction

Geochemists have turned their attention to fluid inclusions as a surviving witness of a past fluid which can reveal something about geological processes. Element and isotopic ratios have been used in classical geochemistry for many decades. In recent years, analytical techniques in geosciences have undergone dramatic improvements. Increased sensitivities and higher precision are pushing down the detection limits, and analyses on individual fluid inclusions are now feasible.

Element ratios on individual inclusions can be measured by laser ablation ICP mass spectrometry (Heinrich et al., 1999; Kamenetsky et al., 1999; Schäfer et al., 1999; Ulrich et al., 1999); at present, measurements of isotopic ratios with this technique have not been performed. Isotope studies are routine for He, Ar, and Sr, and are rapidly approaching feasibility for other systems.

This review will highlight the potential, and the many problems, of radiogenic isotope analyses in fluid inclusions. The questions that can be addressed by isotope studies in fluid inclusions are, in principle, the same that are tackled in macroscopic systems (rocks, minerals): dating and process tracing.

2. Sr isotopes

Dating fluid inclusions by Rb–Sr should be possible, in principle, basing on the assumption that the fluid and the host mineral were in isotopic equilibrium at the time of entrapment. Initial equilibrium fulfills the prerequisite for isochron dating (Faure, 1977, Chapter 6). If the fluid and the mineral subsequently accumulated radiogenic ^{87}Sr, then, in an

* Tel.: +41-31-631-8777; fax: +41-31-631-4988.
E-mail address: igor@mpi.unibe.ch (I.M. Villa).

0024-4937/01/$ - see front matter
PII: S0024-4937(00)00041-4

$^{87}Sr/^{86}Sr$ vs. $^{87}Rb/^{86}Sr$ diagram, the present-day fluid inclusion-host tieline is an isochron giving the age of fluid inclusion formation.

A simple calculation shows what the first big problem is. In a fluid containing 50 ppm Sr, a single $(10\ \mu m)^3$ fluid inclusion contains 10 ng water, or 0.05 pg Sr. Analysing this amount exceeds present analytical capabilities by 4–5 orders of magnitude. In order to increase the amount of Sr available for analysis, it is tempting to pool tens of thousands of inclusions, but this could result in mixing different generations. If the fluid has evolved during its history, such a summation bears the danger of being geologically meaningless. The only viable alternative is, thus, to analyse such minerals that have an unambiguously single generation of fluid inclusions.

Further difficulties are inherent in the extraction technique. An in-depth study (Pettke, 1995; Pettke and Diamond, 1997) has demonstrated that decrepitation has a decisive drawback. Synthetic fluid inclusions with well-known $^{87}Sr/^{86}Sr$ and $^{87}Rb/^{86}Sr$ ratios were decrepitated at various temperatures and analysed. It was observed that the $^{87}Rb/^{86}Sr$ ratio was neither equal to that of the synthesis fluid nor constant, while the $^{87}Sr/^{86}Sr$ ratio was. A possible explanation is that every surface of the system (the decrepitation device and the grain surfaces, especially the freshly cracked ones) adsorbs Rb^+ and Sr^{2+}, but does so differentially. This causes the element fractionation observed by Pettke and Diamond (1997), which, in turn, means that isochron dating by fluid inclusion decrepitation cannot a priori be accurate. While this caution might appear 'hard' on the Rb–Sr technique, it is based on hard experimental facts, which the reader is encouraged to duplicate.

The alternative approach, crushing, suffers from other limitations: some Sr deriving from daughter minerals or from impurities in imperfectly hand-picked separates could contribute a significant bias of the $^{87}Sr/^{86}Sr$ ratio. In summary, the experimental artefacts reported so far discourage Rb–Sr dating, but leave open the possibility to use the $^{87}Sr/^{86}Sr$ ratio as a geochemical tracer. In their study, Pettke and Diamond (1997) argued that the Sr signature of the gold-bearing veins was derived from two reservoirs: the deep auriferous fluid, which had a constant $^{87}Sr/^{86}Sr$ ratio, and wall-rock contamination. They observed (Fig. 1) that wall-rock contamination was greatest in the first crystals forming right after a vein opened and began to be filled; as walls became more and more coated with vein minerals, the $^{87}Sr/^{86}Sr$ ratio in the subsequently grown crystals was different from that of the first ones because it approached that of the deep auriferous fluid; the last generations of vein minerals reached a steady state, suggesting that the wall-rock contamination had become negligible as the wall armouring had become impermeable. The constancy of the $^{87}Sr/^{86}Sr$ ratio is a key argument in the ongoing debate on the genesis of ore

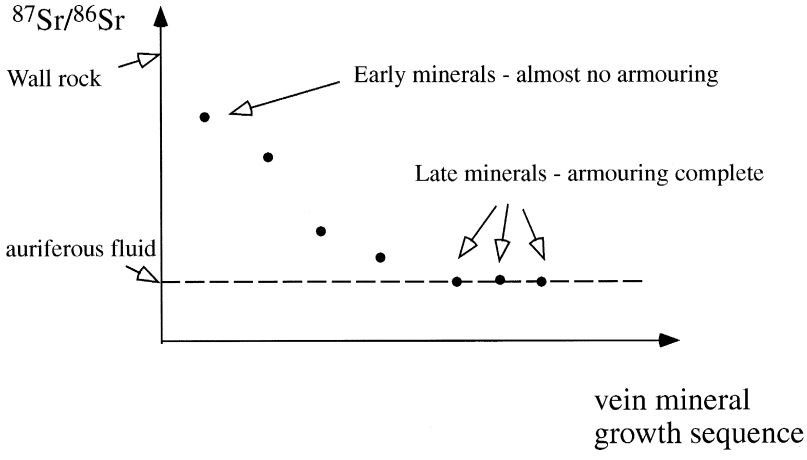

Fig. 1. Evolution of the Sr isotopic composition in fluid inclusions from vein quartz as a function of wall rock armouring (after Pettke and Diamond, 1997).

deposits. The potential of isotopic tracing (in fluid inclusions, or in whole rocks) lies in yielding information which is independent from any element fractionation due to precipitation.

3. Noble gases

Noble gases are one among the many tools used in the past decades to study fluid inclusions.

They are also called 'rare' gases because their abundances in the atmosphere, and hence in air-saturated water, are low: in a $(10\ \mu m)^3$ fluid inclusion filled with air-saturated water at 20°C, there are $2 \cdot 10^{-21}$ moles He, $15 \cdot 10^{-18}$ moles Ar, and $4 \cdot 10^{-22}$ moles Xe. Translated into numbers of atoms, it is clear that He and Xe isotope ratios cannot be measured with any reasonable precision ($^4He = 1200$ atoms, $^3He = 0.002$ atoms, $^{129}Xe \approx {}^{131}Xe \approx {}^{132}Xe \approx 60$ atoms, $^{134}Xe \approx {}^{136}Xe \approx 20$ atoms), but element ratios can. The case of Ar is borderline: $15 \cdot 10^{-18}$ moles Ar contain approximately $5 \cdot 10^{-20}$ moles, or 30,000 atoms, ^{36}Ar. Ideal counting statistics would predict an acceptable uncertainty below 1%; however, present-day mass spectrometers have ionization-plus-transmission efficiencies $< 1\%$, which translates 30,000 atoms to measured count rates of about 1 count/s. Real counting errors depend on the possibility to perform long integrations, i.e. require a high electronic stability; on 1 count/s they exceed tens of percent. In order to increase precision, workers have either analysed larger inclusions (e.g. $(100\ \mu m)^3$) or several thousands of inclusions.

One difficulty inherent in the water–noble gas system is the fractionation by boiling: due to their different kinetic properties, isotopes can be fractionated as a function of mass as soon as the hydrothermal system boils. Because of their quantum-mechanical properties, it is always the heavy isotopes that are enriched in the vapour (see Pettke et al., 1997, and references therein). Boiling appears to have occurred practically always (Rama et al., 1965): in all fluid inclusion measured to date, the $^{40}Ar/^{36}Ar$ ratio is higher than the atmospheric value of 295.5. Incidentally, this means that dating fluid inclusions sensu stricto using radiogenic ^{40}Ar is impossible. Dating cogenetic minerals is an alternative possibility (see below).

3.1. Ar isotopes in fluid inclusions

The extraction of noble gases from fluid inclusions can be achieved by crushing or by decrepitation, the latter either by means of a furnace heating the bulk sample or by a laser melting or vapourizing a few thousands of μm^3 of the mineral.

Crushing has the advantage, and/or disadvantage, of a low efficiency. In-vacuo crushing of a garnet sample by Dunai et al. (1992) released about 1% of the gas contained in the fluid inclusions. Observing the sample after the crushing, it was seen that most grains had remained unbroken because the differential stress was being accommodated by a comparatively small volume fraction of very finely comminuted mineral powder. The necessity of performing the crushing in ultra-high vacuum has so far prohibited stirring and redistributing the mineral in the crusher, which very quickly attains its limits. The low efficiency means that possible daughter phases present in the fluid inclusions are virtually certain to be undamaged, and that the gas release is very selectively restricted to the fluid inclusions. As primary and secondary fluid inclusions are crushed simultaneously, it is necessary to ensure that the sample rigorously contains a single generation of fluid inclusions. The main drawback, however, is that very large amounts of mineral are needed in order to obtain enough gas for an analysis. It is also a cause of concern that the steel surface of the crusher is damaged by hard mineral grains (e.g. quartz) and can become a source of atmospheric Ar for subsequent samples.

Decrepitation by stepwise heating has both advantages and drawbacks. The main problem is certainly the atmospheric blank due to the hot crucible walls, which is higher than in crushing and laser decrepitation (both only require a cold extraction system). High blanks automatically raise the minimum amount of gas needed to achieve a high signal/noise ratio. The main advantage inherent in stepwise heating is the possibility to plot the Ar release as a function of temperature. This allows to separate the degassing bursts of primary and secondary fluid inclusions (which can be directly compared with the results on the same sample obtained on the heating stage) from those of the host and/or daughter minerals, which can be compared with the known differential release

of mineral separates. We shall see examples of both below.

Decrepitation by laser does not suffer from the atmospheric contamination problem, and allows to visually select the area from which to select the fluid inclusions to be analyzed. Due to the violent destruction of the host mineral, it is impossible to separate the gas truly released from fluid inclusions from that released both by the host mineral and that contained in daughter minerals.

Analyzing natural Ar in fluid inclusions gives the $^{40}Ar/^{36}Ar$ ratio, which, in principle, could be used like the $^{87}Sr/^{86}Sr$ ratio to trace the provenance of a fluid. The problem is that the $^{40}Ar/^{36}Ar$ ratio alone is a very poor tracer for two reasons. Firstly, unlike Sr, the mantle and the continental crust have a common Ar isotopic signature: both have higher Ar isotopic ratios than the atmosphere. An ^{40}Ar enrichment is therefore not diagnostic of the fluid's origin. Secondly, volatility makes the Ar concentrations and ratios variable on a very short time-scale (days or weeks); an 'Ar reservoir' is rarely a constant, well-defined entity.

Regarding notation, $^{40}Ar/^{36}Ar$ ratios higher than the atmospheric value of 295.5 are usually called 'radiogenic', even if strictly speaking, the radiogenic

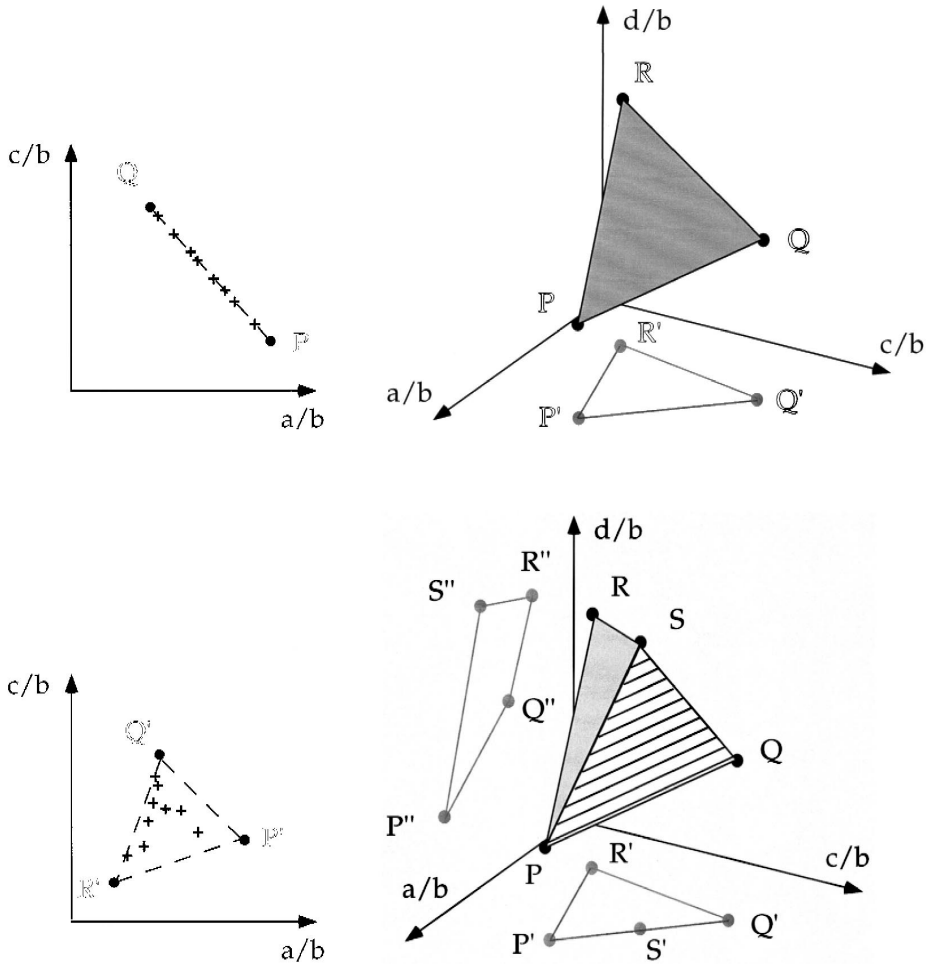

Fig. 2. (a) Binary mixing; (b) two-dimensional view of ternary mixing; (c) three-dimensional view of ternary mixing. The *x–y* plane is identical to Fig. 2b; (d) four-component mixture. Note that two-dimensional projections still resemble triangles, but now corner-points are different in the *x–y* and *x–z* planes.

addition of ^{40}Ar did not occur in situ. The amount of ^{40}Ar which exceeds that accounted for by ^{36}Ar (which is entirely of atmospheric origin) is denoted by an asterisk: thus, $^{40}Ar^{*} = {}^{40}Ar_{total} - {}^{36}Ar \cdot 295.5$.

An important addition to the study of Ar in fluid inclusions is the irradiation technique (known as ^{39}Ar–^{40}Ar in geochronology). Its importance in mineral dating is based on the property of some (but not all) minerals to degas radiogenic and trapped Ar differentially over a finite temperature interval. This allows construction of an internal isochron from several degassing steps as if each step were a different mineral of a cogenetic assemblage in isotopic equilibrium. If an isochron is formed, the unknown initial isotopic ratio can be calculated. In the case of fluid inclusions sensu stricto, this is impossible, as all the Ar is well mixed in the sealed inclusion and is released all at once upon decrepitation. Radiogenic and trapped Ar cannot be resolved from each other. Only if insoluble daughter silicates are formed, and escape any Ar exchange with the fluid subsequently, dating of the latter can be successful (see Fig. 3).

A further characteristic of the ^{39}Ar–^{40}Ar technique is the production of artificial Ar isotopes due to the neutron reactions: ^{39}Ar from K, ^{38}Ar from Cl, and ^{37}Ar from Ca. The 20 possible common-denominator three-isotope correlation diagrams (Hohenberg et al., 1967), such as $^{37}Ar/^{38}Ar$ vs $^{39}Ar/^{38}Ar$, can be used to recognize the components that contribute to the total gas budget.

In the following discussion, we shall use general letters rather than specific isotopic ratios or component names, because the geometrical properties are more profound and equally apply to all isotopic systems. It is easily seen by simple algebra that binary mixing of two components, P and Q, in variable proportions always gives a straight line in a common-denominator three-isotope correlation diagram (Fig. 2a), while ternary mixing P–Q–R will define a triangle in a two-dimensional projection (Fig. 2b) of a plane in a three-dimensional one (Fig. 2c). An example of a binary mixing, such as sketched in Fig. 2a, will be seen in Fig. 4c.

Finally, n components will define an n-polygon in a two-dimensional projection, but will no longer necessarily define a plane in three dimensions if $n > 3$. The example in Fig. 2d shows a fourth component S lying off the plane PQR. The projected vertex, S′, may, however, not always be clearly visible: in this example, the projection onto the x–y plane simulates a three-component system. It is necessary to compare the x–y projection with that on the x–z plane, where S″ is clearly identified as a distinct end member. Applications of Fig. 2d are shown in Figs. 3 and 4d.

The first study, and so far the most successful one, on the source and significance of Ar in fluid inclusions is that by Kelley et al. (1986). These authors examined the components that are a priori expected in fluid inclusions: A = atmospheric Ar (both present-day contamination and Ar dissolved in paleo-groundwaters; K = true radiogenic Ar; E = pure monoatomic (parentless) ^{40}Ar; C = brine with dissolved Ar, Ca, and Cl. In their samples, Kelley et al. (1986) found — as expected — that these four pure end-members formed sample-specific mixtures: M = mixture of C and E; C contains Ar, Cl and Ca in variable proportions, giving rise to two distinct brines in different samples, B and D (Fig. 3). Daughter minerals in the fluid inclusions, or minute micas intergrown with the quartz, allowed dating the hydrothermal system to ≈ 270 Ma.

The example that follows below attempts to combine isotope correlation systematics, differential de-

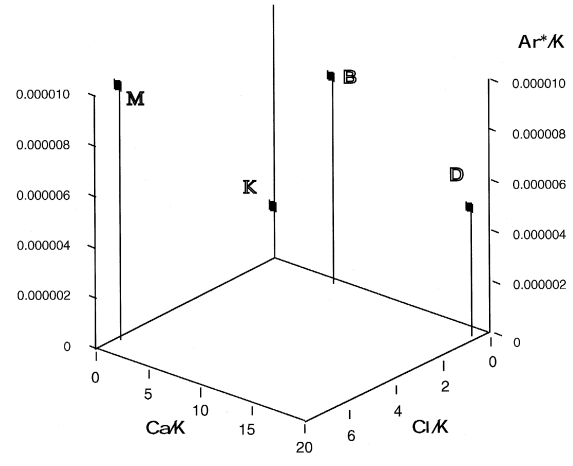

Fig. 3. Multicomponent systematics in fluid inclusions from Cornwall (after Kelley et al., 1986). End-members are: K, radiogenic Ar produced in ≈ 270 Ma; M, mixture of parentless ^{40}Ar and Cl, contained in the saline fluid; D, mixture of parentless ^{40}Ar and Ca; B, a component similar to D, but richer in potassium and parentless ^{40}Ar.

gassing properties, and mass balance considerations. It was presented in preliminary form by Villa et al. (1997). Quartz from the Bruciano borehole in the Larderello geothermal field contains mildly saline aqueous inclusions with CO_2 and subordinate CH_4 and N_2. Ar was analysed in small (≈ 5 mg), hand-picked multi-grain fractions by stepwise heating. Irradiated and unirradiated fractions, I and U, were compared to ensure that no irradiation or interference correction artefact had crept in.

Reproducibility was excellent. Both the relative proportion and the temperature release pattern of $^{40}Ar^*$ was identical (Fig. 4a). A first release pulse, between 400°C and 900°C, may be associated to fluid inclusion decrepitation, as this temperature range is frequently observed under the heating stage (we shall see below how Ar isotopes provide additional support). A second pulse in both I and U is observed at very high temperature.

Artificial production of ^{39}Ar, ^{38}Ar and ^{37}Ar in sample I corresponds to K, Cl and Ca concentrations of 62, 20, and < 10 nmol/g quartz, respectively.

An age calculation was not possible from the fluid inclusion gas alone, because the K contents are very low and the trapped Ar isotopic composition is not atmospheric. Not only fluid inclusions, but also the

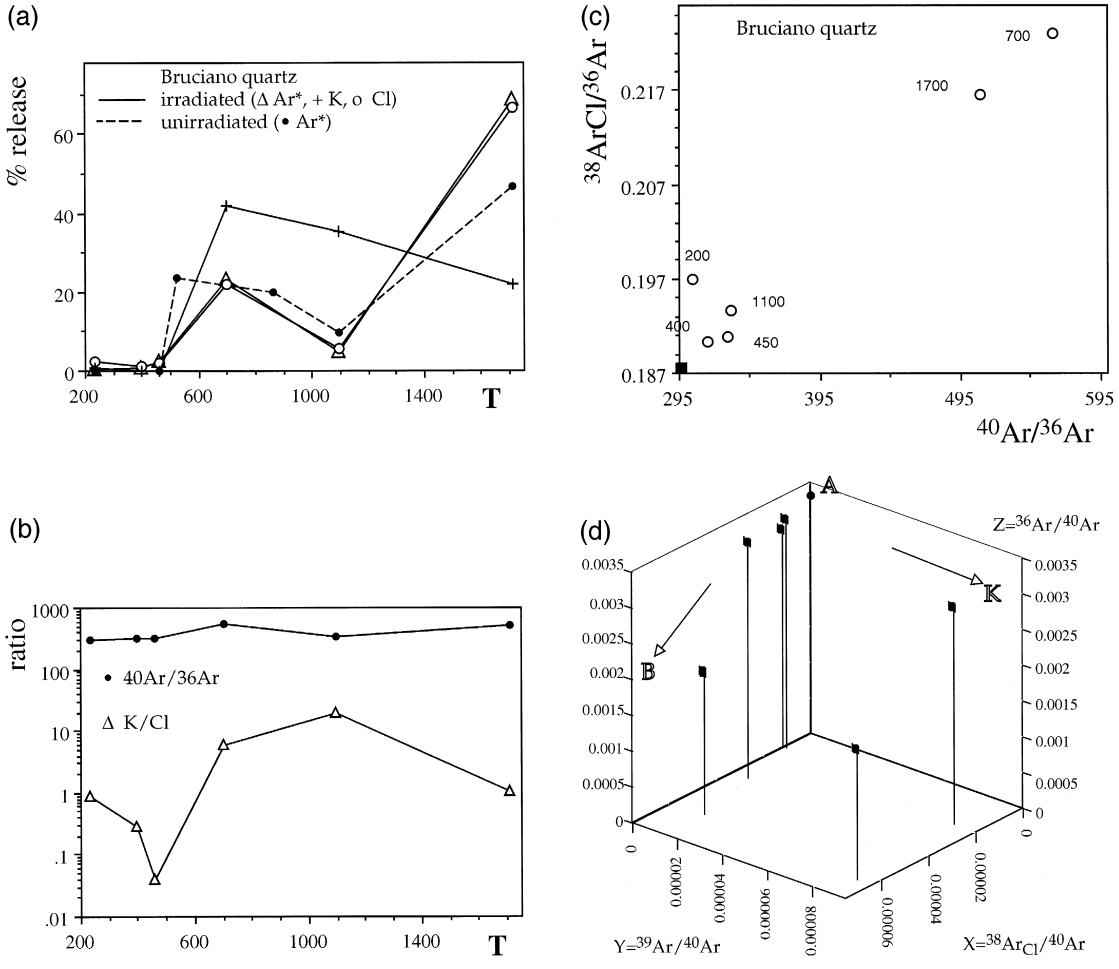

Fig. 4. (a) Differential release of Ar isotopes as a function of temperature; (b) Ar isotopic composition and K/Cl ratio vs. release temperature; (c) three-isotope correlation diagram linking $^{40}Ar^*$ to Cl, i.e. fluid inclusions; (d) three-dimensional isotope correlation similar to Fig. 3d. End-members are: A, atmospheric Ar; B, brine gas, a mixture of parentless ^{40}Ar and Cl; K, radiogenic Ar produced in 5 Ma.

gas from the boreholes, is enriched in $^{40}Ar^*$, which appears to be the rule in the hydrothermal systems reported in the literature.

More encouraging insight is gained from Cl-derived ^{38}Ar. Its release at low temperature ($< 700°C$) points to decrepitation of Cl-bearing fluid inclusions. Our calculated concentration of 20 nmol Cl/g can be exploited as follows. One $(10\ \mu m)^3$ inclusion, 80% aqueous with a 3% salinity, contains 0.4 pmol Cl. Thus, 1 g quartz contains about 50,000 inclusions, which is compatible with visual estimates.

The same mass balance argument, when applied to K, would apparently imply that about 1/3 of the salinity is contributed by K ions. However, we note that the release of K-derived ^{39}Ar is unrelated to that of ^{38}Ar (Fig. 4a–b). In principle, it would be possible that all K is truly contained in the fluid inclusions, but that some ^{39}Ar (which is produced at ≈ 2 MeV by fast neutrons) recoils into the quartz walls and is only degassed at higher temperature, as solid quartz is much more retentive than a decrepitated fluid inclusion. ^{38}Ar is produced by thermal neutrons at much lower energy and undergoes a negligible recoil. Against this interpretation, it can be noted that the K/Cl ratio is low at 1700°C, while selective recoil enrichment of ^{39}Ar in quartz would effect the opposite. Therefore, it is more likely that very little K is in the fluid inclusions, and a different carrier phase is needed. From the degassing temperatures, K-feldspar appears a likely candidate. To account for ≈ 60 nmol/g, the required mass fraction of K-feldspar is 0.002%. Such a low fraction will escape most observers during handpicking.

Finally, from Fig. 4a, it can be seen that the release of Cl-derived ^{38}Ar and $^{40}Ar^*$ is similar. A more rigorous test is given by Fig. 4c, which relates the Cl enrichment (i.e. the $^{38}Ar/^{36}Ar$ ratios above the atmospheric value of 0.187) to the $^{40}Ar^*$ enrichment (i.e. the $^{40}Ar/^{36}Ar$ ratios above 295.5). The slope of the correlation line is the $Cl/^{40}Ar^*$ ratio. It can be seen that this ratio is constant for all steps except the surface-contaminated and very gas-poor 200°C step, which can therefore be discarded. This means that the Cl and the $^{40}Ar^*$ derive from a binary mixture (cf. Fig. 2a) between Ar from the fluid and gas from the mineral host. This implies that there was only one main source of Cl, the fluid inclusion fluid. By extension, the Cl/K ratio then becomes a criterion to discriminate pure fluid inclusion gas from other sources: low Cl/K ratios (e.g. the 1100°C step) are caused by admixture of K unaccompanied by Cl, such as daughter minerals.

The three-dimensional correlation plot is shown in Fig. 4d. With the exception of the 200°C step, the six steps define a plane. This suggests that only three components make up the inventory of the quartz sample: A = atmospheric Ar, B = brine Ar + Cl (from Fig. 4c), K = true radiogenic Ar. The latter, however, lies far off to the right along the *y*-axis, at a value of $^{39}Ar/^{40}Ar \approx 0.2$. By mass balance, its contribution is seen never to exceed 0.04%. The age corresponding to this end-member is ≈ 5 Ma, very close to the known age of hydrothermal systems in Larderello. This agreement may be fortuitous and should not be overinterpreted, because the uncertainty on such a long extrapolation greatly amplifies the uncertainty on the slope of the fit plane.

The implications drawn from this pilot sample are mainly methodological. The heating-stage observation of a single FI generation conforms well with the constant $Cl/^{40}Ar^*$ ratio and the purely binary mixing of Fig. 4c. An age is calculated from the step with highest contribution from daughter minerals, but it is very imprecise.

3.2. Helium

Helium is a less user-friendly tool than Ar. Firstly, it only has two isotopes, ^3He and ^4He. Secondly, the $^4He/^3He$ ratio is 700,000: the instrument for He analysis is required to have detector(s) and electronics with a higher dynamic range than for any other rare gas. Thirdly, He is heavily depleted in the atmosphere and in air-saturated water, making ^3He one of the rarest species in fluid inclusions. He isotopic ratios can only be analyzed from fairly large samples, which contain a population of inclusions. Observation of high or low $^4He/^3He$ ratios alone is not a very stimulating result (Turner et al., 1998). Similarly, analysis of rare gas isotopic ratios in mantle nodule can confirm the mantle provenance (Turner et al., 1990; Frezzotti et al., 1992); however, isotopic data have added little petrologic insight, as rare gases are no pressure indicators and the spread of their isotopic ratios in the mantle is so wide as to preclude a fine diagnosis.

Successful applications of the He system have required combining the He and Ar isotopic and inter-element ratios (Pettke et al., 1997). By stepheating unirradiated metallic gold, these authors were able to decrepitate its fluid inclusions.

Variations in the He–Ar system allow unravelling the sources of rare gases. The Ar/He ratio in the atmosphere is high, and the ratio of two non-radiogenic isotopes $^{36}Ar/^{3}He$ is, thus, very high, 4×10^{6}. The primordial ^{3}He is only preserved in the mantle, which therefore has the lowest $^{4}He/^{3}He$ ratios, $< 10^{5}$, and the lowest $^{36}Ar/^{3}He$, < 30. The radiogenic ingrowth of ^{40}Ar and ^{4}He is highest in the continental crust, which has a high ratio of the radiogenic isotopes, $^{40}Ar/^{36}Ar > 10^{4}$, and $^{4}He/^{3}He > 10^{8}$.

Fig. 5 shows a three-isotope correlation diagram featuring these three terrestrial reservoirs. The main message is to show that three data-points from the analysis of metallic gold and cogenetic quartz (circles and cross) all plot in the left part of the diagram, effectively ruling out any contribution by atmospheric Ar and He. The auriferous fluid had a deep origin (magmatic or metamorphic) and not related to a shallow hydrothermal system open to the atmosphere. The trajectory caused by unmixing by boiling is almost horizontal and could have linked the open and the filled circle. A longer discussion is provided by Pettke et al. (1997, pp. 182–184).

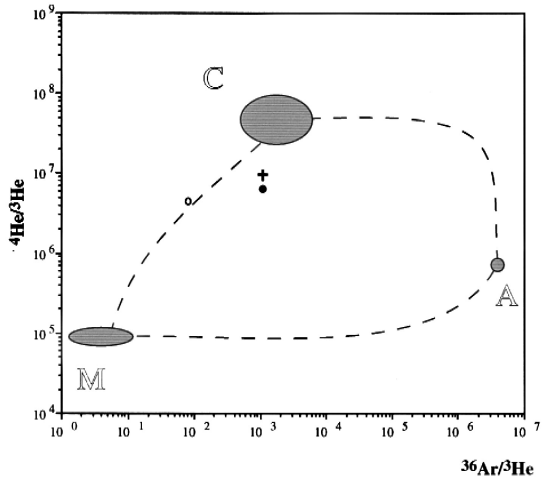

Fig. 5. He–Ar three-isotope correlation diagram. Continental crust (C) and depleted mantle (M) are shown as fields reflecting the uncertain estimates. Air-saturated water (A) does not contribute to the fluid inclusion gas of the Fen 15 sample (circles, cross). The ties between C, M and A are linear as predicted by Fig. 2a–b; their apparent curvature is an effect of the log–log scale.

These authors also used the diathermal decrepitation and the variations in the $^{4}He/^{40}Ar$ ratio to infer the simultaneous presence of vapour-rich and liquid-rich fluid inclusions, deriving from a fluid that underwent unmixing by boiling.

The isotopic data reveal the fluid inclusion inventory of metallic Au, which would otherwise be inaccessible to optical microscopy: not only does Au have fluid inclusions, as had been suspected, but it contains two separate populations.

Further applications of He isotope ratios in fluid inclusions made use of correlations with stable isotopes (Stuart et al., 1994), with Ar isotopes (Burnard and Turner, 1999; Hu et al., 1998) or both (Burnard et al., 1994).

The potential of such a technique lies in tracing the fluid sources and in constraining their genetic processes.

4. Halogens

Halogens Cl, Br and I are certainly rare, but not true noble gases. The reason they are discussed here is that their detection by conventional chemical techniques poses very difficult problems, and the most accessible determination of their concentrations is made via neutron irradiation. One or two noble gas isotopes are produced artificially from each halogen:

^{38}Ar from Cl,
^{80}Kr and ^{82}Kr from Br,
^{128}Xe from I.

These halogen-derived isotopes can be easily detected, because they stick clearly out from the normal terrestrial Ar, Kr and Xe ratios.

Böhlke and Irwin (1992a,b,c) and Irwin (1994) described the analytical procedures and the calibration of production rates.

The technique per se is comparatively unproblematic, although considerable calibration work is required. The main difficulty hampering a widespread use of halogen-produced noble gases in fluid inclusion studies is that the petrological interpretation of

halogen ratios is still in its infancy. The database is growing slowly, and no systematic interpretation of I enrichments or Br depletions in natural systems has been proposed yet.

5. Other isotopic systems

For isotopic systems other than Sr, Ar and He, the present analytical capabilities have not yet reached the point where individual fluid inclusions can be analysed. However, analyses of single-generation fluid inclusion populations are feasible, at least in principle, for other isotopic systems such as Pb. The tracing of fluid inclusion sources is made easier by correlation diagrams, such as Fig. 2. It is important to remember that the curves connecting end members will only be straight lines if the denominator of x and y axes is the same. This is not the case in diagrams, such as, e.g. $^{208}Pb/^{206}Pb$ vs. $^{87}Sr/^{86}Sr$; however, the shape of the tie-curve can be modelled and the spread of the data points still allows recognition of the minimum number of components that make up the mixture.

6. Conclusions

Isotopic tracing is a very powerful tool and allows to reconstruct the origin of fluid inclusion fluids.

On the contrary, dating fluid inclusions is subject to a number of analytical and geochemical artefacts and is unlikely to give reliable ages.

The main reason for caution, as in all scientific experiments, is the need to ask the right question.

Acknowledgements

T. Andersen, T.-L. Knudsen and an unnamed referee are thanked for their reviews.

References

Böhlke, J.K., Irwin, J.J., 1992a. Laser microprobe analyses of noble gas isotopes and halogens in fluid inclusions: analyses of microstandards and synthetic inclusions in quartz. Geochim. Cosmochim. Acta 56, 187–201.

Böhlke, J.K., Irwin, J.J., 1992b. Laser microprobe analyses of Cl, Br, I and K in fluid inclusions: implications for sources of salinity in some ancient hydrothermal fluids. Geochim. Cosmochim. Acta 56, 203–225.

Böhlke, J.K., Irwin, J.J., 1992c. Brine history indicated by Ar, Kr, Cl, Br, and I analyses of fluid inclusions from the Missisippi Valley type lead–fluoride–barite deposits at Hansonburg, New Mexico. Earth Planet. Sci. Lett. 110, 51–66.

Burnard, P.G., Stuart, F., Turner, G., 1994. C–He–Ar variations within a dunite nodule as a function of fluid inclusion morphology. Earth Planet. Sci. Lett. 128, 243–258.

Burnard, P.G., Hu, R.Z., Turner, G., Bi, X.W., 1999. Mantle, crustal and atmospheric noble gases in Ailaoshan gold deposits, Yunnan Province, China. Geochim. Cosmochim. Acta 63, 1595–1604.

Dunai, T.J., Touret, J.L.R., Villa, I.M., 1992. Mantle derived helium in fluid inclusions of a 2.5 Ga old granulite, Nilgiri Hills, India. In: Kharaka, Y.K., Maest, A.S. (Eds.), Water–Rock Interaction. Balkema, Rotterdam, pp. 919–922.

Faure, G., 1977. Principles of Isotope Geology. Wiley, New York, 464 pp.

Frezzotti, M.L., Burke, E.A.J., De Vivo, B., Stefanini, B., Villa, I.M., 1992. Mantle fluids in pyroxenite nodules from Salt Lake Crater (Oahu Hawaii). Eur. J. Mineral. 4, 1037–1053.

Heinrich, C.A., Günther, D., Audetat, A., Ulrich, T., Frischknecht, R., 1999. Metal fractionation between magmatic brine and vapor, determined by microanalysis of fluid inclusions. Geology 27, 755–758.

Hohenberg, C.M., Munk, M.N., Reynolds, J.H., 1967. Spallation and fissiogenic xenon and krypton from stepwise heating of the Pasamonte achondrite; the case for extinct plutonium 244 in meteorites; relative ages of chondrites and achondrites. J. Geophys. Res. 72, 3139–3177.

Hu, R.Z., Burnard, P.G., Turner, G., 1998. Helium and argon isotope systematics in fluid inclusions of Machangqing copper deposit in West Yunnan Province, China. Chem. Geol. 146, 55–63.

Irwin, J.J., 1994. A laser microprobe, mass spectrometric study of Ar, Kr, K, Cl and Br in an "unconformity garnet", associated fluid inclusions, staurolite and micas from Vermont, USA. Chem. Geol. 115, 153–170.

Kamenetsky, V.S., Wolfe, R.C., Eggins, S.M., Mernagh, T.P., Bastrakov, E., 1999. Volatile exsolution at the Dinkidi Cu–Au porphyry deposits, Philippines: a melt-inclusion record of the initial ore-forming process. Geology 27, 691–694.

Kelley, S., Turner, G., Butterfield, A.W., Shepherd, T.J., 1986. The source and significance of Ar isotopes in fluid inclusions from areas of mineralisation. Earth Planet. Sci. Lett. 79, 303–318.

Pettke, Th., 1995, Radiogenic isotopes in fluid inclusions and hydrothermal minerals: methods and application to epigenetic auriferous veins in the Monte Rosa Gold District, NW Italy, PhD Thesis, Universität Bern, 190 pp.

Pettke, Th., Diamond, L.W., 1997. Oligocene gold quartz veins at Brusson, NW Alps: Sr isotopes trace the source of ore-bearing fluid to over a 10-km depth. Econ. Geol. 92, 389–406.

Pettke, Th., Frei, R., Kramers, J.D., Villa, I.M., 1997. Isotope systematics in vein gold from Brusson, Val d'Ayas (NW

Italy). II: (U+Th)/He and K/Ar in native Au and its fluid inclusions. Chem. Geol. 135, 173–187.

Rama, S.N.I., Hart, S.R., Roedder, E., 1965. Excess radiogenic argon in fluid inclusions. J. Geophys. Res. 70, 509–511.

Schäfer, B., Frischknecht, R., Günther, D., Dingwell, D.B., 1999. Determination of trace element partitioning between fluid and melt using LA-ICP-MS analysis of synthetic fluid inclusions in glass. Eur. J. Mineral. 11, 415–426.

Stuart, F.M., Turner, G., Duckworth, R.C, Fallick, A.E., 1994. Helium isotopes as tracers of trapped hydrothermal fluids in ocean-floor sulfides. Geology 22, 823–826.

Turner, G., Burgess, R., Bannon, M., 1990. Volatile-rich mantle fluids inferred from inclusions in diamond and mantle xenoliths. Nature 344, 653–655.

Turner, G., Burnard, P., Pattrick, R., Hu, R., Caligari, A., Hu, R.Z., 1998. Helium and argon in ore fluids: so what? Min. Mag. 62A, 1551–1552.

Ulrich, T., Günther, D., Heinrich, C.A., 1999. Gold concentrations of magmatic brines and the metal budget of porphyry copper deposits. Nature 399, 676–679.

Villa, I.M., Bakker, R., Boiron, M.-C., Cathelineau, M., 1997. $^{39}Ar/^{40}Ar$ analysis of fluid inclusions from the Larderello geothermal field. Abstract, ECROFI 14, Nancy, July 1997, pp. 341–342.